

Precise Positioning of Lubricant on a Surface Using the Local Anodic Oxide Method

Yufei Mo,^{†,‡} Ying Wang,^{†,‡} Jibin Pu,^{†,‡} and Mingwu Bai^{*†}

State Key Laboratory of Solid Lubrication, Lanzhou Institute of Chemical Physics, Chinese Academy of Sciences, Lanzhou 730000, PR China, and Graduate School of the Chinese Academy of Sciences, Beijing 100039, PR China

Received October 13, 2008. Revised Manuscript Received October 29, 2008

This letter describes a new method for the precise positioning of a lubricant on a surface. The nanometer-sized patterns are first fabricated using the atomic force microscopy (AFM)-based local anodic oxide (LAO) method. Multiply alkylated cyclopentanes (MACs) serving as lubricant matrix layers on nanopatterns of silicon dioxide are fabricated. By controlling the velocity of pull-off and solution conditions, we selectively immobilize MACs on the patterned areas using the dip-coating method. In our study, AFM is used for both fabrication and characterization. AFM-LAO allows the fabricated patterns to be altered in situ without the need to change masks or repeat the entire fabrication process. Furthermore, the nanotribological characterization of lubricant matrix layers on the nanopatterns was investigated with a colloidal probe.

Nanostructures and nanodevices have attracted tremendous attention as well as physical challenges in ultimately scaled designs for the future. Patterns with dimension of 100 nm or larger have been fabricated using photolithography,^{1,2} micro-contact printing,^{3–7} microwriting,^{8,9} and micromachining.¹⁰ Ion and electron beam lithography have produced patterns within the films with dimensions of tens of nanometers under ultrahigh vacuum conditions.^{11–13} Scanning probe lithography (SPL), nanoparticle masks, and nanografting have produced patterns with dimensions of several nanometers within self-assembled monolayers (SAMs).^{14–16} The nanopattern SAMs produced via SPL or nanografting have primarily been negative patterns or in solution.^{17–19} The challenging task remains to produce more

nanometer- or molecular-scale patterns with controlled lateral metrology.¹⁸

Local anodic oxidation (LAO) via the atomic force microscope (AFM) is a lithography technique perspective for the fabrication of nanometer-scaled structures and devices.²⁰ AFM-LAO is based on direct oxidation of the sample by negative voltage applied to the AFM tip with respect to the surface of the sample. The AFM-LAO process can be used not only in the fabrication of nanodevices but also in adhesion resistance and friction reduction as surface texturing.²¹ In previous studies, AFM-LAO has been demonstrated to be the most promising tool for fabricating nanodots and lines on several types of materials ranging from metals to semiconductors.^{22–30}

Multiply alkylated cyclopentanes (MACs) are composed of one cyclopentane ring with two to five alkyl groups substituted on the ring. They are synthesized by reacting dicyclopentadiene with alcohols of various chain lengths producing a lubricant with a selective range of physical properties.³¹ Currently, the MAC is a mixture of di- and trisubstituted (2-octylodecyl) cyclopentanes. MAC has excellent viscosity properties, thermal stability, and low volatility for use as a lubricant and is presently gaining wide acceptance on actual space applications.³² Unfortunately, it is difficult to control the size and distribution of

* Corresponding author. Tel: +86-931-4968080. Fax: +86-931-4968163. E-mail: mwbai@lzb.ac.cn.

[†] Lanzhou Institute of Chemical Physics, Chinese Academy of Sciences.

[‡] Graduate School of the Chinese Academy of Sciences.

- (1) Huang, Y. Y.; Dahlgren, D. A.; Herminger, J. C. *Langmuir* **1994**, *10*, 626.
- (2) Tarlov, M. J.; Burgess, D. R.F.; Gillen, G. J. *Am. Chem. Soc.* **1993**, *115*, 5305.
- (3) Lopez, G. P.; Albers, M. W.; Schreiber, S. L.; Carroll, R.; Peralta, E.; Whitesides, G. M. *J. Am. Chem. Soc.* **1993**, *115*, 5877.
- (4) Jeon, N. L.; Nuzzo, R. G.; Xia, Y.; Mrksich, M.; Whitesides, G. M. *Langmuir* **1995**, *11*, 3024.
- (5) Jeon, N.; Lin, W.; Frhardt, M. K.; Girolami, G. S.; Nuzzo, R. G. *Langmuir* **1997**, *13*, 3833.
- (6) Xia, Y.; Whitesides, G. M. *Angew. Chem., Int. Ed.* **1998**, *37*, 550.
- (7) Husemann, M.; Mecerreyes, D.; Hawker, C. J.; Hedrick, J. L.; Shah, R.; Abbott, N. L. *Angew. Chem., Int. Ed.* **1999**, *38*, 647.
- (8) Kumer, A.; Biebuyck, M. A.; Abbott, N. L.; Whitesides, G. M. *J. Am. Chem. Soc.* **1992**, *114*, 9188.
- (9) Abbott, N. L.; Kumar, A.; Whitesides, G. M. *Chem. Mater.* **1994**, *6*, 596.
- (10) Abbott, N. L.; Folkers, J. P.; Whitesides, G. M. *Science* **1992**, *257*, 1380.
- (11) Allara, D. L.; Tiberio, R. C.; Craighead, H. G.; Lercel, M. *Appl. Phys. Lett.* **1993**, *62*, 476.
- (12) Berggren, K. K.; Bard, A.; Wilbur, J. L.; Gillaspay, J. D.; Helg, A. G.; McClelland, J. J.; Rolston, S. L.; Phillips, W. D.; Prentiss, M.; Whitesides, G. M. *Science* **1995**, *269*, 1255.
- (13) Sondag-Huethorset, J. A. M.; Van Helleputte, H. R. J.; Fokkink, L. G. J. *Appl. Phys. Lett.* **1994**, *64*, 285.
- (14) Ross, C. B.; Sun, L.; Crook, R. M. *Langmuir* **1993**, *9*, 632.
- (15) Piner, R. D.; Zhu, J.; Xu, F.; Hong, S. H.; Mirkin, C. A. *Science* **1999**, *283*, 661.
- (16) Mo, Y. F.; Bai, M. W. *J. Phys. Chem. C* **2008**, *112*, 11257.
- (17) Xiao, D.; Liu, G. Y.; Charych, D. H.; Salmeron, M. *Langmuir* **1995**, *11*, 1600.
- (18) Xu, S.; Miller, S.; Laibinis, P. E.; Liu, G. Y. *Langmuir* **1999**, *15*, 7244.
- (19) Wadu-Mesthrige, K.; Xu, S.; Amro, N. A.; Liu, G. Y. *Langmuir* **1999**, *15*, 8580.

(20) Dagata, J. A. *Science* **1995**, *270*, 1625.

(21) Mo, Y. F.; Wang, Y.; Bai, M. W. *Physica E* **2008**, *41*, 146.

(22) Chen, Z.; Hou, S.; Sun, H.; Zhao, X. J. *J. Phys. D: Appl. Phys.* **2004**, *37*, 1357.

(23) Avouris, P.; Hertel, T.; Martel, R. *Appl. Phys. Lett.* **1997**, *71*, 285.

(24) Yang, M.; Zheng, Z.; Liu, Y.; Zhang, B. *Nanotechnology* **2006**, *17*, 330.

(25) Okada, Y.; Amano, S.; Kawabe, M.; Harris, J. S. *J. Appl. Phys.* **1998**, *83*, 7998.

(26) Jian, S. R.; Feng, T. H.; Chuu, D. S. *J. Phys. (Paris)* **2005**, *38*, 2432.

(27) Chien, F. S.; Chang, J. W.; Lin, S. W.; Chou, Y. C.; Chen, T. T.; Gwo, S.; Chao, T. S.; Hsieh, W. F. *Appl. Phys. Lett.* **2000**, *76*, 360.

(28) Xie, X. N.; Chung, H. J.; Xu, H.; Sow, C. H.; Wee, A. T. *Appl. Phys. Lett.* **2004**, *84*, 4914.

(29) Xie, X. N.; Chung, H. J.; Xu, H.; Sow, C. H.; Wee, A. T. *J. Am. Chem. Soc.* **2004**, *126*, 7665.

(30) Lyuksyutov, S. F.; Vaia, R. A.; Paramonov, P. B.; Juhl, S.; Waterhouse, L.; Ralich, R. M.; Sigalov, G.; Sancaktar, E. *Nat. Mater.* **2003**, *2*, 468.

(31) Venier, C. G.; Casserly, E. W. *Lubricants Comprising Novel Cyclopentanes, Cyclopentadienes, Cyclopentenes, and Mixtures Thereof and Methods of Manufacture*. U.S. Patent 4,929,782, 1990.

(32) Dube, M. J.; Bollea, D.; Jones, W. R.; Marrcheti, M.; Jansen, M. J. *Tribol. Lett.* **2003**, *15*, 3.

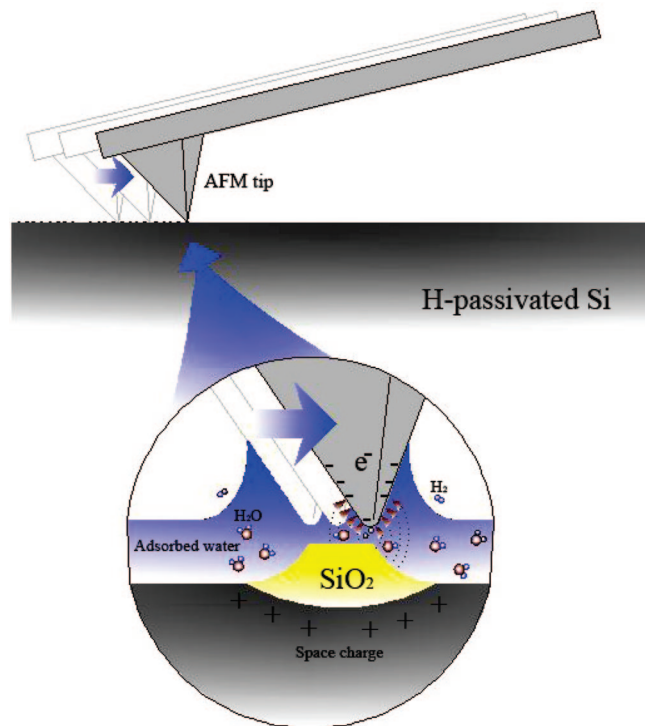


Figure 1. Schematic of the local anodic oxidation process induced by a biased conductive AFM tip.

lubricants precisely on silicon and diamondlike carbon (DLC), which limits their applications in magnetic record storage microelectromechanical systems (MEMS).^{33,34}

Our approach utilizes an AFM-LAO technique to control the size and distribution of lubricants precisely in an atmospheric environment. The nanotribological properties and nanostructures produced in each step are also characterized using AFM. This new technique includes two main steps: the production of nanometer-sized nanopatterns using AFM-LAO, followed by the selective adsorption of MAC lubricant onto these patterns using the dip-coating method. The LAO process performed by AFM is illustrated in Figure 1. The driving force is the faradaic current flows between the tip and sample surface with the aid of the water meniscus. When the faradaic current flows into water bridge, H₂O molecules are decomposed into oxyanions (OH⁻ and O⁻) and protons (H⁺). These ions penetrate into the oxide layer because of the high electric field ($E > 10^7$ V/m),³⁵ leading to the formation and subsequent growth of SiO₂ on the H-passivated Si surface. The H-passivated Si substrate is hydrogen passivated by leaking H₂ into an ultrahigh vacuum (UHV) chamber, where atomic H was created by creaking H₂ molecules on a hot tungsten filament. The process can prevent silicon being converted to a nonuniform native oxide.³⁶ To improve the resolution of oxide nanotexture, we focus on the fabrication of nanotextures on H-passivated Si substrate by LAO.

The LAO process is controlled by several major parameters: pulsed bias voltage, pulse width, and humidity. The height of the oxide can be well controlled by changing these parameters. Figure 2a shows that patterns were fabricated by LAO at a pulse bias voltage of 10 V, a pulse width of 100 ms, and relative humidity

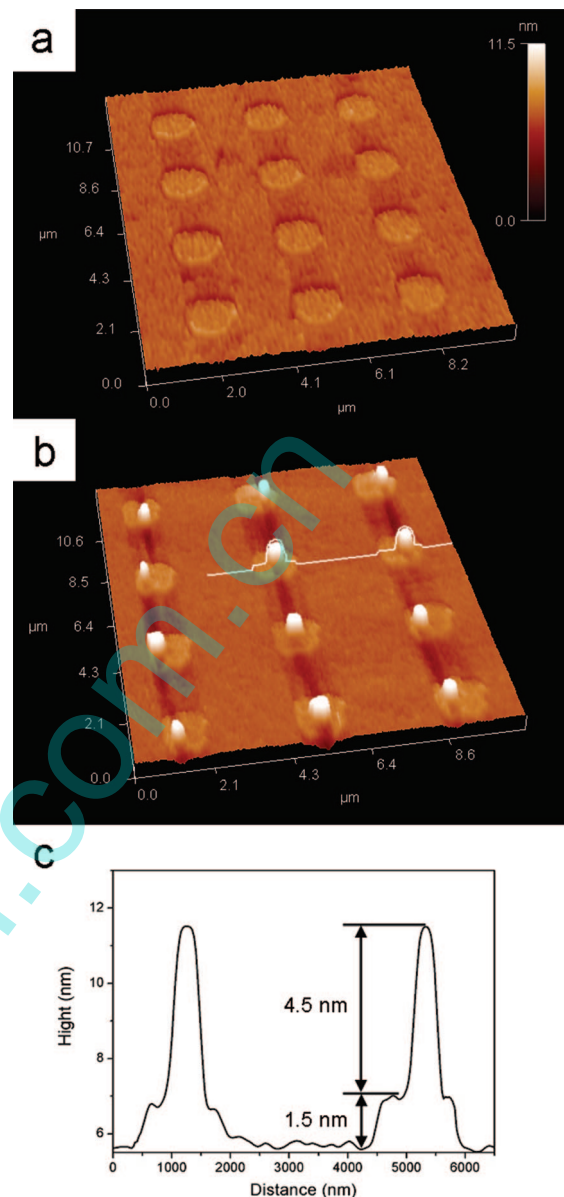


Figure 2. Formation of nanopatterns and MAC lubricant layer: (a) AFM topographic image of patterned H-passivated Si. (b) The same area imaged after being dip-coated in a MAC solution. (c) Corresponding cursor profiles across the MAC nanopatterns. The Ge attenuated total reflective FTIR spectra of the MAC layer on patterned silicon is given in the Supporting Information in Figure S1.

of 20%. The patterned silicon substrate was then dip-coated in a 0.1 mg/mL MAC solution in hexane solvent. After the solvent evaporated, MAC droplets were distributed on the patterns, as shown in Figure 2b. The cursor profile shown in Figure 2c reveals different heights before and after dip-coated MAC. From the Figure, the height of the pattern was about 1.5 nm, and the thickness of the MAC lubricant layer was about 4.5 nm.

For adhesion and friction force measurements of the fabricated patterns, a colloidal probe was prepared by gluing a glass sphere with a radius of 40 μm onto an individual tipless cantilever. The cantilever used in our experiments was etched from single-crystal silicon, and the force constant of the cantilever was calculated using the individually measured thickness, width, and length.³⁷ The above dimensions were determined by a scanning electron microscope, and the normal force constant of the cantilever was

(33) Ma, J. Q.; Liu, J. X.; Mo, Y. F.; Bai, M. W. *Colloids Surf., A* **2007**, *301*, 481.

(34) Ma, J. Q.; Pang, C. J.; Mo, Y. F.; Bai, M. W. *Wear* **2007**, *263*, 1000.

(35) Jian, S. R.; Fang, T. H.; Chuu, D. S. *J. Phys D: Appl. Phys.* **2005**, *38*, 2432.

(36) Ratter, K. A.; Lyding, J. W. *Nanotechnology* **2008**, *19*, 15704.

(37) Liu, Y. H.; Wu, T.; Evans, D. F. *Langmuir* **1994**, *10*, 2241.

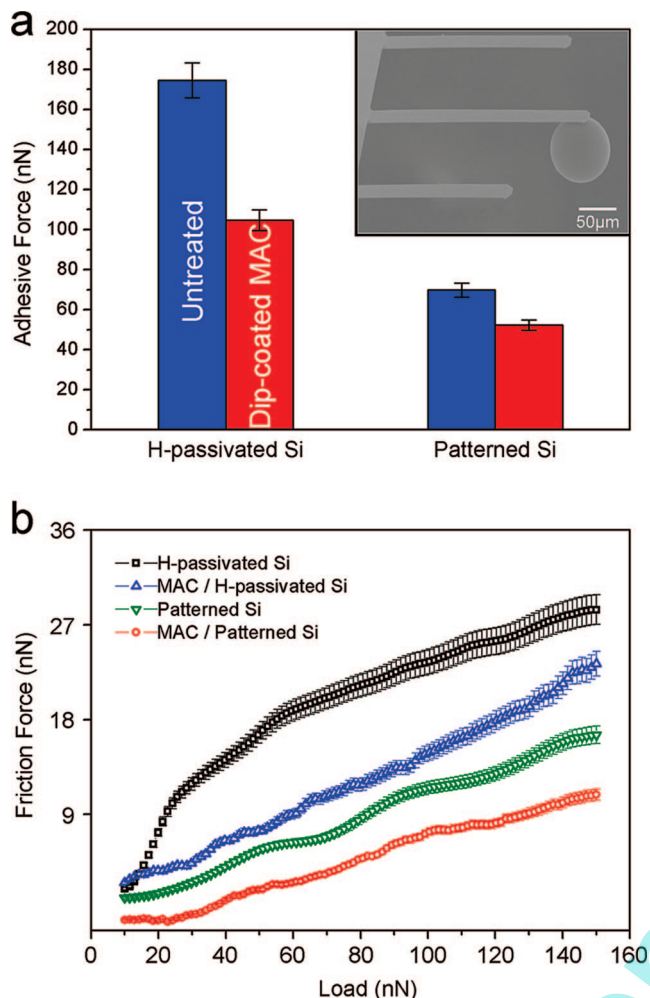


Figure 3. Plots of (a) adhesive forces and (b) friction force between the AFM colloidal probe and the surfaces of samples. The inset shows an SEM image of a typical colloidal probe. More detailed data is given in the Supporting Information in Figure S2.

determined to be 0.275 N/m, which is close to the announced force constant 0.30 N/m. The friction force was calibrated by the method described in ref 38. The inset of Figure 3 shows the SEM image of a typical colloidal probe. The colloidal probe was cleaned sequentially in ethanol and acetone before use. For all measurements, the same cantilever was used in this comparative study.

(38) Bhushan, B. *Handbook of Micro/Nano Tribology*, 2nd ed.; CRC Press: Boca Raton, FL, 1994.

Furthermore, to avoid the influence of molecules that may transfer to the tip in the AFM/FFM experiments, the tip was scanned on a cleaved mica surface to remove these physically adsorbed molecules. The relative humidity was controlled at 20%. Repeated measurements were within 5% of the average value for each sample. The adhesive force between the colloidal probe and sample surfaces is shown in Figure 3a. A strong adhesive force was observed on the untreated H-passivated silicon surface, on which the adhesive force was about 175 nN. After the patterns were generated, the adhesive force was decreased to 70 nN. This indicates that the pattern exhibited adhesion resistance. Adhesion is directly related to the bearing ratio, which describes the real area of contact between two solid surfaces.³⁹ After dip-coating in MAC solution, the adhesive forces of untreated H-passivated and patterned Si were decreased to 105 and 52 nN, respectively. Such a phenomenon indicates that the MAC layer on the sample surface can obviously lower the interfacial energy and capillarity between the tip and surface. Figure 3b presents the plot of friction versus load curves for the bare H-passivated Si and patterned Si and these surfaces treated with MAC. Patterned Si evidently reduced the friction force, and the MAC-cover-patterned Si exhibited the lowest friction force whereas H-passivated Si had a strong friction force. The decrease in the friction force is mainly due to a pattern giving rise to a smaller contact area for the same applied load and MAC as the lubricant layer minimizes the shearing strength during sliding.

In summary, nanometer-sized lubricant patterns can be produced using AFM-LAO and the dip-coating method. Regular patterns were fabricated on an H-passivated Si substrate using the AFM-LAO process. Subsequently, the patterned Si substrates were dip-coated in MAC solution. This new positioning of the lubricant method is currently being tested using various lubricants. The strength of our approach is the ability to engineer and image patterned Si and lubricant patterns with nanometer precision. These nanostructures shall provide a unique opportunity for the exploration of chemical and biochemical reactions under a spatially well-defined, controlled environment.

Acknowledgment. This work was funded by the National Natural Science Foundation of China (NSFC) under grant number 20773148 and National 973 Program 2007CB607601.

Supporting Information Available: GATR-FTIR spectra of MAC and force–distance curves. This material is available free of charge via the Internet at <http://pubs.acs.org>.

LA803379E

(39) Marchon, B.; Vierk, S.; Heiman, N.; Fisher, R.; Khan, M. *Tribology and Mechanics of Magnetic Storage Systems*; STLE Special Publication SP-26; STLE: Park Ridge, IL, 1985; Vol. VI.